JOURNAL OF CHEMOMETRICS
J. Chemometrics **13,** 311–329 (1999)

ESTIMATING RATE CONSTANTS AND PURE UV-VIS SPECTRA OF A TWO-STEP REACTION USING TRILINEAR MODELS

SABINA BIJLSMA, D. J. LOUWERSE (AD) AND AGE K. SMILDE*
Process Analysis and Chemometrics, Department of Chemical Engineering, University of Amsterdam, Nieuwe Achtergracht 166, NL-1018 WV Amsterdam, The Netherlands

SUMMARY

This paper describes the estimation of reaction rate constants and pure species UV-vis spectra of the consecutive reaction of 3-chlorophenylhydrazonopropane dinitrile with 2-mercaptoethanol. The reaction rate constants were estimated from the UV-vis measurements of the reacting system using the generalized rank annihilation method (GRAM) and the Levenberg–Marquardt/PARAFAC (LM-PAR) algorithm. Both algorithms can be applied in cases where the contribution of different species in the mixture spectra is of exponentially decaying character. From a single two-way array, two two-way datasets are formed by means of splitting such that there is a constant time lag between the two two-way datasets. By stacking these two two-way datasets, the reaction rate constants can be estimated very easily from the third dimension. GRAM, which is fast and non-iterative, decomposes the trilinear structure using a generalized eigenvalue problem (GEP). The iterative algorithm LM-PAR consists of a combination of the Levenberg–Marquardt algorithm and alternating least squares steps of the PARAFAC model using GRAM results as a set of initial starting values. Pure spectra of the absorbing species were estimated and compared with their measured pure spectra. LM-PAR performed the best, giving the lowest relative fit error. However, the relative fit error obtained with GRAM was acceptable. Since a lot of measurements are based on exponentially decaying functions, GRAM and LM-PAR can have many applications in chemistry. Copyright © 1999 John Wiley & Sons, Ltd.

KEY WORDS: UV-vis; jackknife; GRAM; LM-PAR; kinetics

INTRODUCTION

Estimation of reaction rate constants is a necessary procedure for the determination of reaction mechanisms. In chemical kinetics the course of a reaction is very often monitored at specific wavelengths where only one reacting species absorbs.[1,2] However, this approach is only applicable for reaction systems where the spectra of the different species involved are not overlapping and hence a high degree of selectivity is present. Problems arise if spectra of different species are similar or overlapping. In such a situation it is very hard to find a wavelength where only the non-interesting species have a very small absorption coefficient. Chemometric methods which can deal with overlapping spectra of reacting species would be the most convenient solution for such problems. Nowadays computerized data processing is widely used in scientific research, and complicated data-processing techniques can be used.

* Correspondence to: A. K. Smilde, Process Analysis and Chemometrics, Department of Chemical Engineering, University of Amsterdam, Nieuwe Achtergracht 166, NL-1018 WV Amsterdam, The Netherlands.

CCC 0886–9383/99/030311–19 $17.50

Received 15 June 1998
Accepted 5 November 1998

One of these techniques is curve resolution[3] based on the determination of qualitative information and recovery of response profiles, e.g. time profiles. A large number of curve resolution techniques have been published.[4–6] Curve resolution techniques can also be used to deconvolute spectral features using a model for the kinetic information. Reaction rate constants can be incorporated as unknowns.[7–9] An iterative least squares optimization procedure is used to estimate the values of unknown reaction rate constants from experimental data of the reaction. Also hard-modelling methods such as global analysis,[10–12] can be used to estimate kinetic parameters and equilibrium parameters from multiwavelength spectral data.

However, time-consuming iterations can be a serious problem if such procedures are used to estimate parameters on-line from batch processes in industry. An iterative procedure is therefore not very attractive to use and a fast non-iterative algorithm could be applied to monitor the considered chemical process. The non-iterative algorithm need not to be very accurate, because a rough estimate of parameters is very often satisfactory. If the batch time is elapsed, an iterative algorithm can be used to estimate reaction rate constants more accurately.

In recent work[13] a non-iterative algorithm, which is a modification of the generalized rank annihilation method (GRAM) based on the direct exponential curve resolution algorithm (DECRA) developed by Windig and Antelek,[14,15] has been used in order to estimate reaction rate constants from the short-wavelength near-infrared (SW-NIR)[16,17] spectra of a reacting system. This modified GRAM method can only be used in cases where the contribution of different species in the mixture spectra is of exponentially decaying character. Kinetic equations have an exponentially decaying character[13] and hence it is possible to estimate reaction rate constants using GRAM. GRAM can only be used for (pseudo-)first-order kinetics. In the modified GRAM method a single dataset of a reacting system is split into two datasets by means of a time shift such that there is a constant time lag between the two datasets. Owing to the properties of exponentially decaying functions, there exists a special trilinear structure if the two datasets are stacked. This trilinear structure is decomposed by solving a generalized eigenvalue problem (GEP).[18] From the decomposition, specific parameters, e.g. reaction rate constants, can be estimated.

Recently a new iterative algorithm has been developed[13] for cases where very accurate estimations of reaction rate constants are needed. The iterative algorithm, called Levenberg–Marquardt/PARAFAC (LM-PAR), is a combination of the well-known Levenberg–Marquardt algorithm[19] and alternating least squares steps of the PARAFAC model[20,21] using the GRAM results as a very good set of initial starting values.

In previous work,[13] GRAM and LM-PAR have been applied in order to estimate the reaction rate constants from short-wavelength near-infrared (SW-NIR) measurements of the pseudo-first-order two-step epoxidation of 2,5-di-*tert*-butyl-1,4-benzoquinone[8,22] and from simulated datasets. A quality assessment of the estimated reaction rate constants was performed using the jackknife method.[23] Both algorithms can deal with strong spectral overlap. The experimental data showed only a small difference between GRAM and LM-PAR estimations of the reaction rate constants. Simulations showed that LM-PAR always leads to more precise estimates of the reaction rate constants compared with GRAM. The choice of the time shift parameter appeared to be very important. A small time shift results in two datasets which are very similar, and a large time shift results in two very small datasets. Both cases will result in very bad estimations for the kinetic parameters. For instance, the reaction rate constants can become very large or even negative or a complex number.

Goal of the paper

In this paper, GRAM and LM-PAR are applied in order to estimate reaction rate constants from UV-

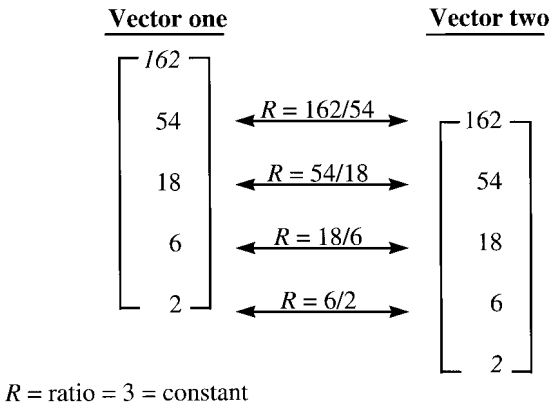

Figure 1. Relation between a vector with exponentially decaying numbers (vector one) and the corresponding shifted vector (vector two)

vis measurements of the two-step consecutive reaction of 3-chlorophenylhydrazonopropane dinitrile with 2-mercaptoethanol.[2,24] The choice of the time shift parameter is also investigated. The pure spectra of the reacting species, including an intermediate species, which absorb in the considered UV-vis region are estimated very easily, without complicated procedures, and compared with their measured pure spectra. If species are unknown, spectrum library search methods can be used to identify the estimated pure spectra of these unknown species. Quality assessment of the estimated reaction rate constants is also performed using the jackknife method.

THEORY

In a previous paper[13] the model, algorithms and quality assessment of the estimated reaction rate constants were explained very extensively. Here those three items will be explained very briefly.

Notation

Boldface capital characters denote matrices, boldface lower-case characters denote vectors, boldface underlined capital characters denote a three-way array and the superscript 'T' denotes a transpose. $\mathbf{A}^{(j)}$ is the matrix $\mathbf{A}$ after the jth iteration and $\mathbf{a}_i$ is the ith column of $\mathbf{A}$. Hence $\mathbf{a}_i^{(j)}$ is the ith column of $\mathbf{A}$ after the jth iteration. In the Appendix there is a summary of the nomenclature of the most important scalars, vectors and matrices used in this paper.

The model

Shifting an exponentially decaying function

Let a vector of exponentially decaying numbers, called vector one, be equal to $[162 \quad 54 \quad 18 \quad 6 \quad 2]^{\mathrm{T}}$. Next suppose vector one is shifted one position, which results in vector two according to Figure 1. From this figure it is clear that the ratio R between two numbers listed in the same row is equal from row to row. In this case the ratio equals three.

Equation (1) represents an exponentially decaying function describing the reaction kinetics of a

first-order process.

$$C = \mathrm{e}^{-k_1 t} \tag{1}$$

where k_1 is a reaction rate constant and C is the concentration of a certain species at time t. If the exponent is shifted with a time shift S, equation (1) becomes equation (2).

$$C_\mathrm{s} = \mathrm{e}^{-k_1(t+S)} \tag{2}$$

where C_s is the 'shifted concentration'. The ratio of equations (1) and (2), called λ, is an indirect measure for k_1 as shown in equation (3).

$$\lambda = \frac{C}{C_\mathrm{s}} = \frac{\mathrm{e}^{-k_1 t}}{\mathrm{e}^{-k_1(t+S)}} = \mathrm{e}^{-k_1 t + k_1(t+S)} = \mathrm{e}^{k_1 S} \quad \Leftrightarrow \quad k_1 = \frac{\ln(\lambda)}{S} \tag{3}$$

Hence, if an exponentially decaying function is time-shifted, the reaction rate constant can be extracted very easily from the ratio of the non-shifted and the shifted exponentially decaying function.

The reaction model

Suppose that the following first-order consecutive reaction is considered as the reaction model.

Step 1. A $\rightarrow$ B, with reaction rate constant k_1.
Step 2. B $\rightarrow$ C, with reaction rate constant k_2.

Then equations (4)–(6) are the kinetic rate equations describing the concentration profiles of species A, B and C respectively with initially only A present.

$$C_{\mathrm{A},i} = C_{\mathrm{A},0}\mathrm{e}^{-k_1 t_i} \tag{4}$$

$$C_{\mathrm{B},i} = \frac{k_1 C_{\mathrm{A},0}}{k_2 - k_1}(\mathrm{e}^{-k_1 t_i} - \mathrm{e}^{-k_2 t_i}) \tag{5}$$

$$C_{\mathrm{C},i} = C_{\mathrm{A},0} - C_{\mathrm{A},i} - C_{\mathrm{B},i} \tag{6}$$

where $C_{\mathrm{A},i}$, $C_{\mathrm{B},i}$ and $C_{\mathrm{C},i}$ are the concentrations of species A, B and C at time t_i respectively and $C_{\mathrm{A},0}$ is the initial concentration of species A at the starting point of the reaction.

Let matrix $\mathbf{X}$ ($M \times N$) be a collection of spectra taken during a certain time course with M equidistant time points at N wavelengths of a reacting system in which K species are involved. In curve resolution, matrix $\mathbf{X}$ can be expressed as equation (7) assuming Lambert–Beer's law.[16]

$$\mathbf{X} = \mathbf{F}\mathbf{D}^\mathrm{T} + \mathbf{E} \tag{7}$$

The matrices from equation (7) have the following properties.

1. Every row in $\mathbf{X}$ denotes a spectrum recorded at a certain time.
2. $\mathbf{F}$ ($M \times K$) is the matrix of concentration profiles.
3. Every column in $\mathbf{F}$ denotes the concentration profile of a species in time. Hence every column in $\mathbf{F}$ represents a rate equation.

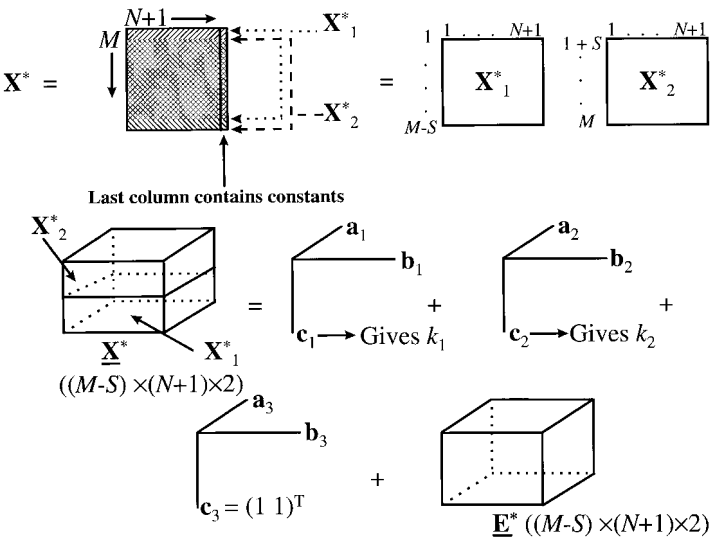

Figure 2. PARAFAC model

4. **D** ($N \times K$) is the matrix containing the pure spectra of the species.
5. Every column in **D** represents the pure spectrum of a species.
6. **E** ($M \times N$) is the matrix of errors (model errors, experimental errors and instrumental noise).

The trilinear structure

Consider the two reactions from the reaction model described above and matrix **X** ($M \times N$) with UV-vis measurements of the reacting system. Suppose for convenience that $C_{A,0} = 1$. Equations (4 and 5) are already sums of exponentially decaying functions, but equation (6) is not decaying. It is necessary for a combination of exponentially decaying functions to be modelled with GRAM or LM-PAR that these functions can be written as a sum of exponentially decaying components.[13] Hence, using equations (4 and 5), equation (6) can be rewritten.

$$C_{C,i} = 1 - e^{-k_1 t_i} - k(e^{-k_1 t_i} - e^{-k_2 t_i}) = e^0 - e^{-k_1 t_i} - ke^{-k_1 t_i} + ke^{-k_2 t_i} \tag{8}$$

where $k = k_1/(k_2 - k_1)$. Now equation (8) is a sum of individual exponentially decaying functions. Although the term e^0 is implicitly present in the dataset, it is advantageous (certainly in the case of noisy data) to add a column of constants, e.g. $(1 \quad \ldots \quad 1)^T$ (a column with ones), to the data matrix **X** ($M \times N$) to construct an augmented data matrix $\mathbf{X}^*$ ($M \times (N+1)$).[25,26]

Next $\mathbf{X}^*$ will be used to build two data matrices $\mathbf{X}^*_1$ and $\mathbf{X}^*_2$ using a time shift S. The matrices $\mathbf{X}^*_1$ ($(M - S) \times (N+1)$) and $\mathbf{X}^*_2$ ($(M - S) \times (N+1)$) formed by separating $\mathbf{X}^*$ are used to construct the three-way array $\underline{\mathbf{X}}^*$ ($(M - S) \times (N+1) \times 2$) by stacking and can be modelled with PARAFAC as shown in Figure 2. From the three-way array $\underline{\mathbf{X}}^*$ the following three loading matrices can be constructed:

- $\mathbf{A} = [\mathbf{a}_1\ \mathbf{a}_2\ \mathbf{a}_3]$ ($(M - S) \times 3$) with k-rank[27] equal to three
- $\mathbf{B} = [\mathbf{b}_1\ \mathbf{b}_2\ \mathbf{b}_3]$ ($(N+1) \times 3$) with k-rank equal to three

- $\mathbf{C} = [\mathbf{c}_1 \ \mathbf{c}_2 \ \mathbf{c}_3]$ (2×3) with *k*-rank equal to two, assuming $k_1 \neq k_2$.

Because a column of constants is added to matrix **X**, the third column of **C** is forced to be equal to one even if **X** contains a lot of noise.

The *k*-rank is defined as follows. Suppose a matrix has *K* columns. If any combination of *L* columns of the matrix is independent and this is not valid for $L + 1$, then the *k*-rank of the matrix is equal to *L*. The three-way rank of $\underline{\mathbf{X}}^*$, called *R*, equals three in this case. For the decomposition of the three-way array in the matrices **A, B** and **C** to be unique, the Kruskal criterion[28] has to be fulfilled. According to the Kruskal criterion, the decomposition is unique if equation (9) is valid.

$$k\text{-rank}(\mathbf{A}) + k\text{-rank}(\mathbf{B}) + k\text{-rank}(\mathbf{C}) \geq 2R + 2 \tag{9}$$

In this case $(3 + 3 + 2) \geq (2 \times 3 + 2) \Rightarrow 8 \geq 8$ and hence the decomposition of the three-way array is unique.

The algorithms

Non-iterative algorithm: the generalized rank annihilation method (GRAM)

In this subsection, GRAM will be explained very briefly starting from the decomposition of the three-way array $\underline{\mathbf{X}}^*((M - S) \times (N + 1) \times 2)$.

Step 1. Start with a GEP. This gives the three loading matrices **A, B** and **C**.[18] In order to solve the GEP, the matrices $\mathbf{X}^*_1$ and $\mathbf{X}^*_2$ need to be transformed into square matrices. This can be done by using a common space[18] on to which both matrices are projected. In this paper the common space was based on $\mathbf{X}^*_1 + \mathbf{X}^*_2$.

Step 2. Recognize the triad which is constant and permute the model such that the third triad models the constant. The reaction rate constants k_1 and k_2 can be estimated directly from the scaling factors listed in the first two columns of the **C** matrix, according to equation (10), if the time shift is known using equation (3).

$$\mathbf{C} = \begin{pmatrix} u & v & 1 \\ 1 & 1 & 1 \end{pmatrix} \tag{10}$$

where k_1 and k_2 are ln $(u)/S$ and ln $(\nu)/S$ respectively.

Iterative algorithm: the Levenberg–Marquardt algorithm and alternating least squares steps of the PARAFAC model (LM-PAR)

LM-PAR, which is monotonically decreasing, will be explained in this subsection very briefly. For all the estimates obtained with LM-PAR in this paper, the GRAM results were used as a set of initial starting values.

Steps 1 and 2 of LM-PAR are equal to GRAM. Let the three matrices **A, B** and **C** obtained from the first step of GRAM be $\mathbf{A}^{(0)}$, $\mathbf{B}^{(0)}$ and $\mathbf{C}^{(0)}$ respectively. Let the estimated k_1 and k_2 obtained by the second step of GRAM be start-k_1 and start-k_2 respectively. The superscript zero indicates that no iterations have occurred yet.

Step 3. Define $\tilde{\mathbf{A}}^{(0)}$ which is a matrix with the reconstructed exponentially decaying functions using start-k_1 and start-k_2 for k_1 and k_2 respectively. Define $\tilde{\mathbf{C}}^{(0)}$ which is equal to $\mathbf{C}^{(0)}$. Define $\tilde{\mathbf{B}}^{(0)}$ which is a least squares PARAFAC fit from the three-way array $\underline{\mathbf{X}}^*$, $\tilde{\mathbf{C}}^{(0)}$ and $\tilde{\mathbf{A}}^{(0)}$.

Step 4. Subtract the contribution of the column with constants from the three-way array $\underline{\mathbf{X}}^*$:

$$\tilde{\underline{\mathbf{X}}}^{*(0)} = \underline{\mathbf{X}}^* - \mathbf{a}_3^{(0)}(\mathbf{c}_3^{(0)\mathrm{T}} \otimes \tilde{\mathbf{b}}_3^{(0)\mathrm{T}}) \tag{11}$$

Step 5. Next matrices are partitioned:

$$\tilde{\mathbf{A}}^{(0)} = [\tilde{\tilde{\mathbf{A}}}^{(0)}, \mathbf{a}_3^{(0)}]$$
$$\tilde{\mathbf{C}}^{(0)} = [\tilde{\tilde{\mathbf{C}}}^{(0)}, \mathbf{c}_3^{(0)}] \quad \text{with } \mathbf{c}_3^{(0)} = \begin{pmatrix} 1 \\ 1 \end{pmatrix}$$
$$\tilde{\mathbf{B}}^{(0)} = [\tilde{\tilde{\mathbf{B}}}^{(0)}, \tilde{\mathbf{b}}_3^{(0)}]$$

Step 6. Equation (12) is minimized over k_1 and k_2 using the Levenberg–Marquardt algorithm, ensuring that for the proper k_1 and k_2 this minimum will be attained.

$$\min_{k_1,k_2} ||\tilde{\underline{\mathbf{X}}}^{*(0)} - \tilde{\tilde{\mathbf{A}}}^{(0)}(\tilde{\tilde{\mathbf{C}}}^{(0)^{\mathrm{T}}} \otimes \tilde{\tilde{\mathbf{B}}}^{(0)^{\mathrm{T}}})||^2 \tag{12}$$

Hence $\tilde{\tilde{\mathbf{A}}}^{(0)}$ and $\tilde{\tilde{\mathbf{C}}}^{(0)}$ are updated simultaneously using the optimal values for k_1 and k_2 according to the Levenberg–Marquardt algorithm.

Step 7. Update $\tilde{\mathbf{B}}^{(0)}$ using a least squares PARAFAC step.

Step 8. Repeat Steps 4–7 until the relative change in fit between two iterations is below 10^{-6}.

Estimation of the relative fit error

If the reaction rate constants are estimated with GRAM or LM-PAR, the fit error can be estimated. In this paper this was done in the following way. Unfold the three-way matrix $\underline{\mathbf{X}}^*$ and the estimate of $\underline{\mathbf{X}}^*$, $\hat{\underline{\mathbf{X}}}^*$, according to equation (13), and delete the two columns with constants to construct $\bar{\mathbf{X}}$ ($(M - S) \times 2N$) and $\bar{\hat{\mathbf{X}}}$($(M - S) \times 2N$) respectively.

$$\hat{\underline{\mathbf{X}}}^* = \tilde{\mathbf{A}}(\tilde{\mathbf{C}}^{\mathrm{T}} \otimes \tilde{\mathbf{B}}^{\mathrm{T}}) \tag{13}$$

where $\tilde{\mathbf{A}}$, $\tilde{\mathbf{B}}$ and $\tilde{\mathbf{C}}$ are obtained with GRAM or LM-PAR.

The relative fit error (RFE) can be estimated according to equation (14).

$$\mathrm{RFE} = \sqrt{\frac{\sum_{i=1}^{j}\sum_{j=1}^{j}(\bar{\mathbf{X}} - \bar{\hat{\mathbf{X}}})_{ij}^2}{\sum_{i=1}^{I}\sum_{j=1}^{J}\bar{\mathbf{X}}_{ij}^2}} \tag{14}$$

where $I = M - S$, $J = 2N$, $i = 1, 2, \ldots, I$ and $j = 1,2, \ldots,J$. From equation (14) it can be seen that it is necessary to delete the columns with constants from the two-way arrays, because otherwise the denominator will dominate.

Estimation of the pure spectra

For a set of estimated reaction rate constants obtained with GRAM or LM-PAR, the concentration profiles are reconstructed. From these concentration profiles and the original UV-vis spectra from the considered batch run, the pure spectra of reactant, intermediate and product can be estimated by means of a fast non-negativity-constrained least squares algorithm.[29] The absorbances of these estimated pure spectra are relative absorbances and hence have to be scaled for comparison with the measured pure spectra.

Quality assessment of the estimated reaction rate constants

If the reaction rate constants are estimated, there will be a certain fluctuation between the several estimated parameters. This can be caused by model errors, experimental errors and instrumental noise. The model errors can be kept very small if the correct kinetic model is used and the Lambert–Beer law is valid. Experimental errors are always present and are caused by concentration errors and errors due to the start of the reaction, for example. Instrumental noise is also always present and is caused by variations in the instrument. If reaction rate constants are estimated for several repeated individual batch processes and the individual standard deviation is estimated, this represents the upper error limit. Note that this is the worst case, because both experimental errors and instrumental noise are involved.

A lower error limit caused by mainly instrumental noise is estimated using the jackknife method. The theory of the jackknife method is very well explained in the book by Shao and Tu.[23] Consider the mean batch run obtained from averaging all the repeated individual batch process runs. Hence experimental errors and also instrumental noise are averaged. In the jackknife procedure a fixed number of spectra from the three-way array $\underline{\mathbf{X}}^*$ based on the mean batch run are left out several times according to a fixed interval, and hence the three-way array $\underline{\mathbf{X}}^*$ is reduced.[13] Finally for the mean batch process a set of estimates for the reaction rate constants are obtained. The individual standard deviation of these estimates represents the lower error limit, because mainly instrumental noise is involved.

EXPERIMENTAL

The reaction

The two-step consecutive reaction of 3-chlorophenylhydrazonopropane dinitrile (A), an uncoupler of oxidative phosphorylation in cells, with 2-mercaptoethanol (B) described by Bisby and Thomas[2] and Chau and Mok[24] was used as an example process for experiments. The two chemicals form an intermediate adduct (C) which is hydrolysed in an apparently intramolecular reaction to the product 3-chlorophenylhydrazonocyanoacetamide (D) and the by-product ethylene sulphide (E). A possible reaction mechanism is given in Figure 3.

$$\mathrm{A} + \mathrm{B} \xrightarrow{k_1} \mathrm{C} \xrightarrow{k_2} \mathrm{D} + \mathrm{E}$$

If 2-mercaptoethanol is present in large excess, pseudo-first-order kinetics can be assumed. Hence the kinetic equations (4)–(6) can be used to describe the concentration profiles of A, C and D respectively. In this paper, A, C and D will be monitored— the reactant, intermediate and main product of the considered reaction.

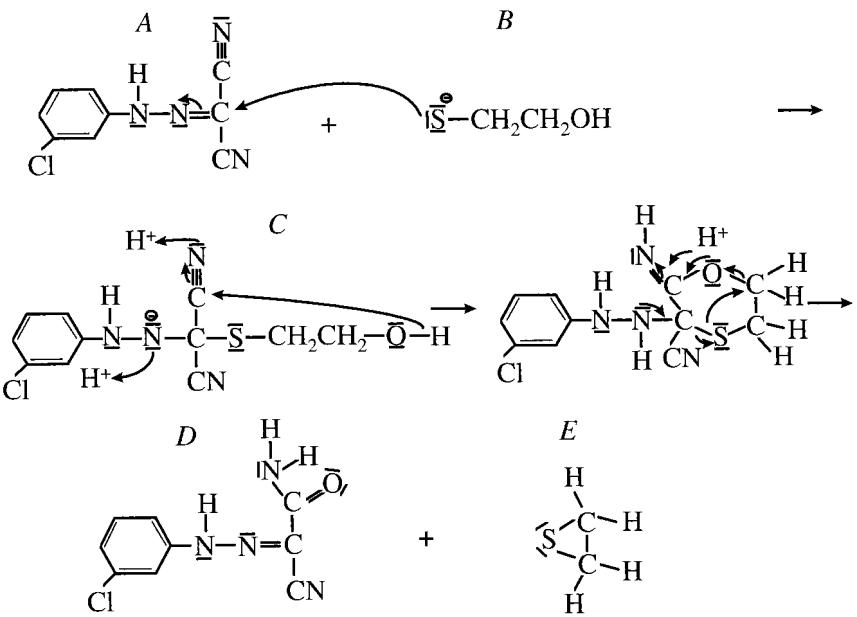

Figure 3. Proposed reaction mechanism: A, 3-chlorophenylhydrazonopropane dinitrile; B, 2-mercaptoethanol; C, intermediate adduct; D, 3-chlorophenylhydrazonocyanoacetamide; E, ethylene sulphide

Sample preparation

All chemicals were used as received without further purification. 0·0529 g (0·2585 mmol) of species A (Acros, 99+%) was dissolved in water using a minimum amount of 0·1 mol l^{-1} of NaOH (Baker Chemicals, 98·8%) to give a stock solution of 1·034 mmol l^{-1}. This stock solution was diluted into a working solution containing 51·71 μmol l^{-1} of species A, buffered with KH_2PO_4 (Acros, pro analysis 0·2 mol l^{-1}, pH 4·4). This working solution had to be prepared freshly every day. At this pH, species A was supersaturated and slowly crystallized from the solution after a couple of days. This was not observed by Bisby Thomas[2] and Chau and Mok.[24] The cuvette was filled with 2·5 ml of the working solution. When the temperature inside the cuvette had reached the target temperature of 25 °C, data collection was started upon addition of 10 μl of a B solution, which contained 35·65 μmol of species B, by means of a pipette. This B solution consisted of 250 μl of pure B (Acros, 99%) and 750 μL of KH_2PO_4 buffer solution. However, if pure B is added, it will take some time to mix with the reaction mixture. This mixing time can be reduced if B is already in the same buffer solution as the buffer solution used to create the reaction mixture. The excess of B in moles was 276 times A.

Pure spectra

Seven spectra were recorded of the reaction mixture for the case where no B was added. Hence the recorded spectra represented the measured pure spectrum of the reactant when the buffer solution was used as blank. In order to record the pure spectrum of the product, the reaction mixture was allowed to react for about 8 h. After this reaction period, seven spectra were recorded. Hence the recorded spectra represented the measured pure spectrum of the product when the buffer solution was used as blank. After 8 h the concentrations of the reactant and intermediate are negligible. It is not possible to record the pure spectrum of the intermediate. Bisby and Thomas[2] tried to record the pure spectrum of

Table 1. Most important experimental conditions

Reaction temperature	25 °C
Integration time[a]	1 s
Sampling time	10 s
Total run time	2700 s
Wavelength range	200–600 nm
Wavelength interval	1·0 nm
Number of recorded spectra	271

[a] It took 1 s to measure ten spectra from 200 to 600 nm. These spectra were averaged.

the intermediate immediately after addition of B. This is not correct, because the reaction will start directly. Bisby and Thomas mentioned this problem too, but were satisfied with an approximate pure spectrum of the intermediate. In this paper such an approach will be useless, because 'the measured pure spectrum' cannot be compared with the estimated pure spectrum if the 'measured pure spectrum' is not the real pure spectrum.

Experimental set-up

The experimental set-up has been extensively described in an earlier paper.[13] A Hewlett Packard 8453 UV-vis spectrophotometer with diode array detection was used to measure spectra of the reacting system. In this paper a quartz cuvette with 1·00 cm path length was used to obtain spectra of the reaction mixture. A Pt-100 and a constant-temperature bath (Neslab) were used to control the temperature inside the cuvette. The most important experimental conditions are given in Table 1.

Reproducibility

The reproducibility R_{batch} of ten individual batch process runs was obtained using equation (15).[9,30]

$$R_{\text{batch}} = \frac{\sqrt{\frac{1}{n}\sum_{i=1}^{n} ||\mathbf{X}_i - \mathbf{X}_m||^2}}{||\mathbf{X}_m||} \times 100\% \tag{15}$$

where $\mathbf{X}_i$ is the data matrix for process run i and $\mathbf{X}_m$ is the averaged data matrix estimated for n individual batch process runs according to equation (16).

$$\mathbf{X}_m = \frac{1}{n}\sum_{i=1}^{n} \mathbf{X}_i \tag{16}$$

The reproducibility R_{time} for every recorded spectrum at time t was obtained according to equation (17).

$$R_{\text{time}(t)} = \frac{\sqrt{\frac{1}{n}\sum_{i=1}^{n} ||\mathbf{x}_{i,t} - \mathbf{x}_{m,t}||^2}}{||\mathbf{x}_{m,t}||} \times 100\% \tag{17}$$

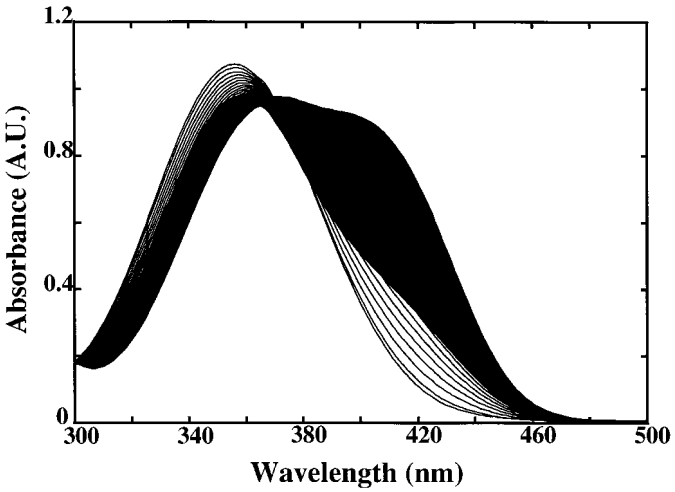

Figure 4. Blank-corrected UV-vis spectra recorded during one individual batch process run for wavelength range 300–500 nm

where $\mathbf{x}_{i,t}$ is the spectrum for process run i at time t and $\mathbf{x}_{m,t}$ is the averaged spectrum m at time t estimated for n individual batch process runs according to expression (18).

$$\mathbf{x}_{m,t} = \frac{1}{n}\sum_{i=1}^{n} \mathbf{x}_{i,t} \tag{18}$$

Data processing

A spectrum of the KH_2PO_4 buffer solution was used as blank solution. The reproducibility of each recorded spectrum was calculated in order to decide whether some spectra had to be deleted because of bad reproducibility caused by mixing of the B solution at the start of the reaction. Only a selection of the wavelength range was used for data processing. At $\lambda < 300$ nm, species B absorbs and by-product E shows an increasing absorbance. At $\lambda > 500$ nm there is no significant contribution of the reacting species to the absorbance. If the wavelength range 300–500 nm is considered, the spectral features are caused by A, C and D.

Data processing was performed in the Matlab environment (Version 4·2C, The Mathworks Inc.) on a Pentium 133 MHz computer with 64 MB RAM and a 1·2 GB hard disk.

RESULTS AND DISCUSSION

Reproducibility

The blank-corrected spectra of one arbitrary individual batch process run are shown in Figure 4. The reproducibility of the batch process runs was 0·54%, which is very good for spectroscopic measurements. The reproducibility for every spectrum in time is shown in Figure 5. From this figure it is clear that the first spectrum had to be deleted because of the poor reproducibility compared with the other reproducibility numbers.

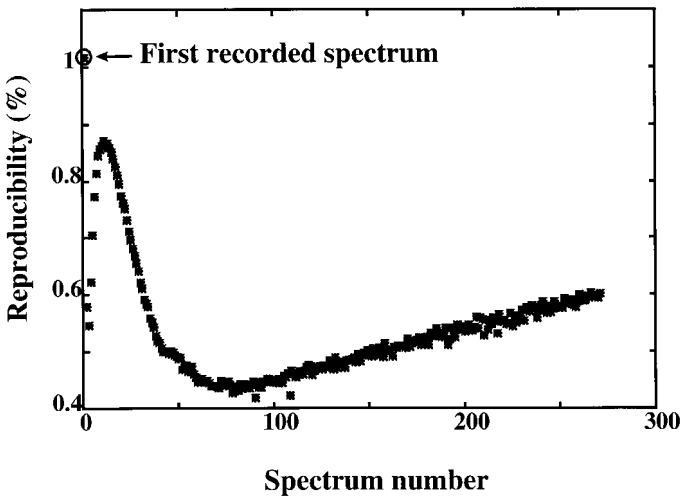

Figure 5. Reproducibility versus spectrum number

Effect of the time shift on the reaction rate constant estimates

In order to investigate the effect of different time shifts, the kinetic parameters were estimated for ten repeated individual batch processes with GRAM for different time shifts. A time shift of $S = 1$ or one datapoint means a time shift of one spectrum. The results are listed in Table 2. From this table the following aspects can be observed.

1. A small time shift results in large individual standard deviations for both k_1 and k_2. A large time

Table 2. Mean estimated reaction rate constants and individual standard deviations (STDs) obtained with GRAM and different time shifts for ten repeated individual batch process runs

Time Shift	Mean k_1 (min^{-1})	STD k_1 (min^{-1})	Mean k_2 (min^{-1})	STD k_2 (min^{-1})
1	0·3129	0·0239	0·0267	0·0075
2	0·3083	0·0159	0·0280	0·0048
3	0·3062	0·0129	0·0287	0·0036
4	0·3052	0·0112	0·0290	0·0028
5	0·3050	0·0104	0·0291	0·0023
6	0·3048	0·0098	0·0291	0·0020
7	0·3047	0·0094	0·0291	0·0018
8	0·3046	0·0091	0·0291	0·0017
9	0·3047	0·0089	0·0291	0·0015
10	0·3047	0·0087	0·0291	0·0015
20	0·3052	0·0083	0·0286	0·0011
30	0·3040	0·0083	0·0284	0·0010
40	0·3019	0·0091	0·0282	0·0010
50	0·3006	0·0093	0·0280	0·0009
60	0·2995	0·0099	0·0280	0·0008
70	0·2971	0·0096	0·0279	0·0008
80	0·2945	0·0096	0·0279	0·0008

Table 3. Individual estimated reaction rate constants for ten repeated individual batch process runs and mean batch process run. The values were obtained with GRAM. The values in parentheses were obtained with LM-PAR. The mean values ($\bar{k}_1$ and $\bar{k}_2$) and individual standard deviations (STDs) based on the ten individual estimated kinetic parameters from batch numbers 1–10 are also given

Number of batch run	Estimated k_1 (min^{-1})	Estimated k_2 (min^{-1})
1	0·3006 (0·3106)	0·0287 (0·0263)
2	0·3009 (0·3117)	0·0288 (0·0261)
3	0·3040 (0·3117)	0·0285 (0·0264)
4	0·3137 (0·3192)	0·0280 (0·0262)
5	0·3069 (0·3093)	0·0265 (0·0263)
6	0·2932 (0·3070)	0·0298 (0·0262)
7	0·2985 (0·3230)	0·0297 (0·0246)
8	0·3180 (0·3244)	0·0275 (0·0260)
9	0·3109 (0·3304)	0·0277 (0·0232)
10	0·2936 (0·3002)	0·0285 (0·0265)
GRAM	$\bar{k}_1$ = 0·3040, STD = 0·0083	$\bar{k}_2$ = 0·0284, STD = 0·0010
LM-PAR	$\bar{k}_1$ = 0·3147, STD = 0·0092	$\bar{k}_2$ = 0·0258, STD = 0·0011
Mean batch run	0·3038 (0·3146)	0·0284 (0·0258)

shift results in a large individual standard deviation for k_1 and a small individual standard deviation for k_2.

2. A moderate time shift of 30 datapoints is a compromise, because this gives the lowest standard deviation for k_1 and a compromise in standard deviation for k_2.

An important feature is the computation time of reaction rate constants using GRAM or LM-PAR. In this case, GRAM takes only a few seconds but LM-PAR takes a few hours to perform the necessary iterations, approximately 4000–5000. Hence GRAM is very fast.

Estimation of the upper error limit

The individual estimates of the kinetic parameters for each repeated individual batch process and the mean batch process are listed in Table 3 for a time shift of 30 datapoints. The mean batch process was obtained by averaging ten repeated individual batch process runs. GRAM and LM-PAR were both used. The individual standard deviations represent the upper error limit. From Table 3 the following aspects can be observed.

1. If the individual standard deviations are considered, there is no gain in standard deviation when LM-PAR is used instead of GRAM. Both methods perform approximately the same. The mean value for k_1 is higher for LM-PAR than for GRAM. For the k_2 estimates the opposite is valid. Because there is a correlation between the two reaction rate constants, higher k_1 values tend to occur with lower k_2 values.
2. The spread of the k_1 estimates is larger than the spread of the k_2 estimates. Figure 6 shows the reconstructed concentration profiles for species. A, C and D when k_1 and k_2 obtained with LM-PAR for the mean batch process run were used.

For the reaction rate constant estimates of the mean batch process run obtained with both GRAM and LM-PAR, the relative fit error was estimated as described in the Theory section. The relative fit error was $1{\cdot}9 \times 10^{-3}$ for GRAM and $2{\cdot}8 \times 10^{-4}$ for LM-PAR, indicating that the reaction model proposed fits very well. The relative fit error is reduced when LM-PAR is used instead of GRAM.

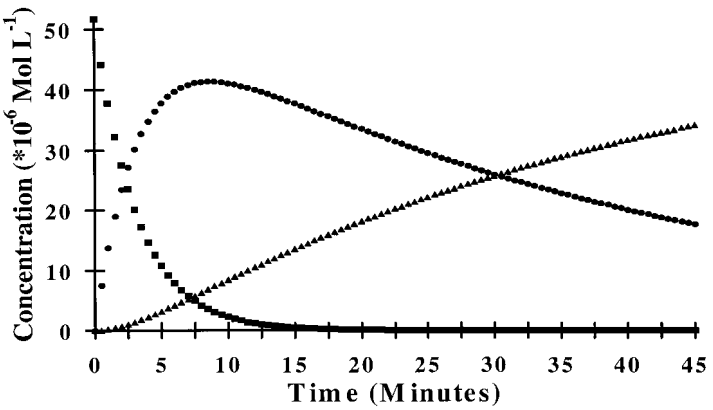

Figure 6. Concentration profiles of reactant (■), intermediate (●) and product (▲) for $k_1 = 0{\cdot}3146$ min^{-1} and $k_2 = 0{\cdot}0258$ min^{-1} obtained with LM-PAR for mean batch process run

Despite the larger relative fit error for GRAM compared with LM-PAR, GRAM can be used to estimate reaction rate constants very fast.

Estimation of the lower error limit

The jackknife procedure described briefly in the Theory section was used to estimate the lower error limit. The jackknife interval was chosen equal to 25. Finally this resulted in ten jackknife estimations for k_1 and k_2 for the mean batch process run. The jackknife procedure was applied for both algorithms. The time shift was again equal to 30 datapoints. The mean estimated kinetic parameters based on ten jackknife estimations and the corresponding standard deviations (lower error limits) obtained with both algorithms are listed in Table 4. From Table 4 it is clear that the use of LM-PAR leads to a decrease in the influence of instrumental error for both k_1 and k_2 estimates.

Estimation of the pure spectra

For the k_1 and k_2 estimation by both algorithms for the mean batch process run, the pure spectra of the species were estimated. Figure 7 shows the estimated pure spectrum for the reactant, using GRAM and LM-PAR results for the reaction rate constants to construct the concentration profiles, and the measured pure spectrum. Figures 8 and 9 show the same situation as in Figure 7 for the intermediate and product respectively. In Figure 8 the measured pure spectrum for the intermediate is not shown,

Table 4. Results from jackknife procedure of mean batch process run. The mean kinetic parameters are the mean values over ten jackknife estimations. The individual standard deviations (STDs) represent the lower error limit. A time shift of 30 datapoints was used. The values were obtained with GRAM. The values in parentheses were obtained with LM-PAR

Mean k_1 (min^{-1})	STD k_1 (min^{-1})	Mean k_2 (min^{-1})	STD k_2 (min^{-1})
0·3037	$1{\cdot}5425 \times 10^{-4}$	0·0284	$4{\cdot}1912 \times 10^{-5}$
(0·3146)	$(9{\cdot}8398 \times 10^{-5})$	(0·0258)	$(1{\cdot}0852 \times 10^{-5})$

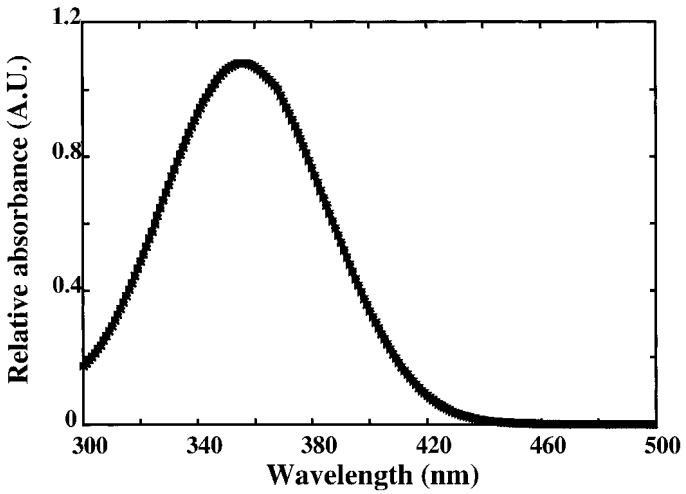

Figure 7. Estimated pure spectra of reactant using GRAM (—) and LM-PAR (∗∗∗) and measured pure spectrum (○○○)

because this spectrum was not available. From Figures 7 and 9 it is clear that the estimated pure spectra, using LM-PAR results for the reaction rate constants, show very small differences from the measured pure spectra. Because the estimated pure spectra of the reactant and product show very small differences from the measured pure spectra and the fits of the models are very good, it can be assumed that the estimated pure spectrum of the intermediate will be very close to the real pure spectrum of the intermediate.

Figure 10 shows differences between estimated pure spectra and measured pure spectra. Figure 10a shows the difference between the estimated pure spectrum and the measured pure spectrum for the reactant, where the estimated pure spectrum was obtained using the results from GRAM to

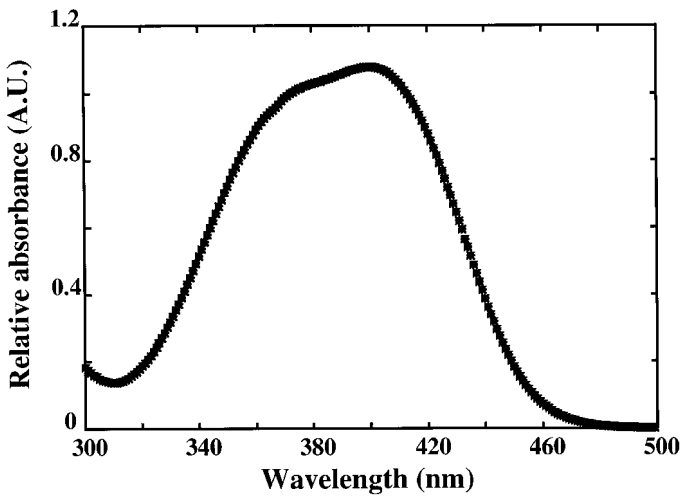

Figure 8. Estimated pure spectra of intermediate using GRAM (—) and LM-PAR (∗∗∗)

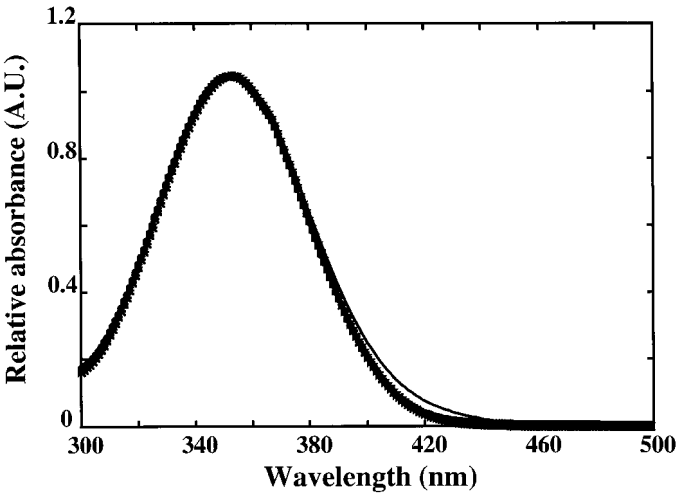

Figure 9. Estimated pure spectra of product using GRAM (—) and LM-PAR (∗∗∗) and measured pure spectrum (○○○)

reconstruct the concentration profiles. Figure 10b shows the same situation as in Figure 10a for LM-PAR. Figures 10c and 10d show the same situation as in Figures 10a and 10b respectively for the product. From Figure 10 it is clear that LM-PAR estimation of the reaction rate constants leads to estimates of pure spectra which are closer to the measured pure spectra compared with the GRAM results.

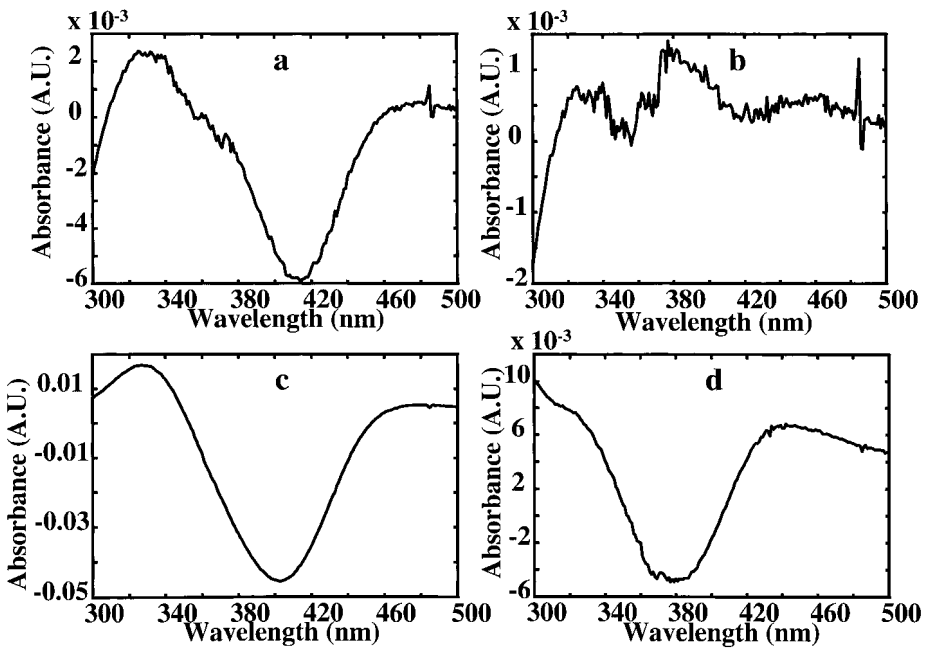

Figure 10. Differences between estimated and measured pure spectra of reactant using GRAM (a), reactant using LM-PAR (b), product using GRAM (c) and product using LM-PAR (d)

Summary of results

A time shift of 30 datapoints appeared to give the lowest individual standard deviation for k_1 and a compromise in individual standard deviation for k_2 when GRAM was used. For all the different batch process runs the reaction rate constants were obtained with both GRAM and LM-PAR for this time shift of 30 datapoints. The individual standard deviations showed that there is hardly any difference in performance between GRAM and LM-PAR. For the mean batch process run the reaction rate constants were estimated with both algorithms. The relative fit errors were $1{\cdot}9 \times 10^{-3}$ and $2{\cdot}8 \times 10^{-4}$ for GRAM and LM-PAR respectively. These values indicate that the kinetic model proposed fitted the best using LM-PAR. However, the fit error value for GRAM is still acceptable. The jackknife procedure showed that the influence of the instrumental error for both reaction rate constants with LM-PAR is lower compared with GRAM and the estimates are reliable.

Finally the pure spectra were estimated for LM-PAR and GRAM results of the reaction rate constants obtained from the mean batch process run. The pure spectra of the reactant and product showed very good agreement with the measured pure spectra. The estimated pure spectrum of the intermediate could not be compared with the measured pure spectrum, because a measured pure spectrum of the intermediate was not available. The difference between estimated pure spectra and measured pure spectra is smaller for reaction rate constants obtained by LM-PAR compared with those obtained by GRAM.

CONCLUSION

In this paper it is shown that GRAM can be used as a very fast non-iterative algorithm in order to estimate reaction rate constants from the UV-vis spectra of the two-step consecutive reaction of 3-chlorophenylhydrazonopropane dinitrile with 2-mercaptoethanol. GRAM takes only a few seconds. The individual standard deviations for the reaction rate constants are comparable with those obtained by LM-PAR, but GRAM gives a larger fit error. LM-PAR can be used in situations where an accurate estimation of reaction rate constants is desirable and there is enough time available to perform the tedious iterations (approximately 4000–5000) which characterize the LM-PAR algorithm. A time shift of 30 datapoints appeared to be optimal for this application. This has to be established in practice again for other kinetic model systems.

When the estimated pure spectra of the absorbing species involved in the reaction model are compared with the measured pure spectra, the difference is very small. LM-PAR gives better estimates for the pure spectra than GRAM. However, GRAM can be used in practice to obtain estimates of reaction rate constants very fast. Using these estimates, the pure spectra can be estimated very easily, without complex procedures.

ACKNOWLEDGEMENTS

The authors acknowledge Professor Dr G.-J. Koomen and R. L. W. Haenraets for the helpful discussion about the possible reaction mechanism.

APPENDIX: NOMENCLATURE

In general, boldface capital characters denote matrices and boldface lower-case characters denote vectors. Table 5 summarizes the nomenclature of some important scalars, vectors and matrices used in this paper.

Table 5. Nomenclature

Variable	Description
$\mathbf{A}$ $((M-S) \times 3)$	Matrix of concentration profiles obtained from a GEP
$\mathbf{A}^{(j)}$ $((M-S) \times 3)$	Matrix $\mathbf{A}$ after jth iteration
$\tilde{\mathbf{A}}$ $((M-S) \times 3)$	New matrix $\mathbf{A}$ obtained by an initial estimate for k_1 and k_2
$\tilde{\mathbf{A}}$ $((M-S) \times 2)$	First two columns of matrix $\tilde{\mathbf{A}}$
$\mathbf{a}_i$	ith column of matrix $\mathbf{A}$
$\mathbf{a}_i^{(j)}$	ith column of matrix $\mathbf{A}$ after jth iteration
$\mathbf{B}$ $((N+1) \times 3)$	Matrix of combined spectra obtained from a GEP
$\mathbf{C}$ (2×3)	Matrix of scaling factors obtained from a GEP
$C_{\mathrm{A,O}}$	Initial concentration of species A
$C_{\mathrm{A},i}$	Concentration of species A at time point i ($C_{\mathrm{B},i}$ and $C_{\mathrm{C},i}$ for B and C respectively)
$\mathbf{D}$ $(N \times K)$	Matrix of pure spectra
$\mathbf{E}$ $(M \times N)$	Matrix of errors
$\underline{\mathbf{E}}^*$ $((M-S) \times (N+1) \times 2)$	Three-way array of errors
$\overline{\mathbf{F}}$ $(M \times K)$	Matrix of concentration profiles
k_1, k_2	Reaction rate constants
k	Equals $k_1/(k_2 - k_1)$
$\overline{k}_1$, $\overline{k}_2$	Mean estimated k_1 and k_2
S	Time shift parameter
T (superscript)	Transpose of a matrix or vector
t_i	Time at point i
$\mathbf{X}$ $(M \times N)$	Matrix of spectra during a certain time course
$\mathbf{X}^*$ $(M \times (N+1))$	Augmented data matrix
$\mathbf{X}^*{}_1$ $((M-S) \times (N+1))$	Data matrix 1 formed by splitting $\mathbf{X}^*$
$\mathbf{X}^*{}_2$ $((M-S) \times (N+1))$	Data matrix 2 formed by splitting $\mathbf{X}^*$
$\underline{\mathbf{X}}^*$ $((M-S) \times (N+1) \times 2$	Three-way array formed by stacking $\mathbf{X}^*{}_1$ and $\mathbf{X}^*{}_2$
$\overline{\overline{\mathbf{X}}}$ $((M-S) \times 2N)$	Matrix obtained by unfolding $\underline{\mathbf{X}}^*$ and deleting the two columns with constants
$\hat{\overline{\mathbf{X}}}$$((M-S) \times 2N)$	Estimate of $\overline{\mathbf{X}}$
$\mathbf{X}_i$ $(M \times N)$	Data matrix of process run i
$\mathbf{x}_{i,\,j}$ $(1 \times N)$	Spectrum of process run i at time t
$\mathbf{X}_m$ $(M \times N)$	Averaged data matrix for n individual batch process runs
$\mathbf{x}_{m,\,t}$ $(1 \times N)$	Averaged spectrum m at time t for n individual batch process runs

REFERENCES

1. L. Drobnica and E. Sturdik, *Biochim. Biophys. Acta*, **585**, 462 (1979).
2. R. H. Bisby and E. W. Thomas, *J. Chem. Educ.* **63**, 990 (1986).
3. W. H. Lawton and E. A. Sylvestre, *Technometrics*, **13**, 617 (1971).
4. R. Tauler, S. Fleming and B. R. Kowalski, *Anal. Chem.* **65**, 2040 (1993).
5. R. Tauler, A. K. Smilde, J. M. Henshaw, L. W. Burgess and B. R. Kowalski, *Anal. Chem.* **66**, 3337 (1994).
6. R. Tauler, A. Izquierdo-Ridorsa, R. Gargallo and E. Casassas, *Chemometrics Intell. Lab. Syst.* **27**, 163 (1995).
7. E. A. Sylvestre, W. H. Lawton and M. S. Maggio, *Technometrics*, **16**, 353 (1974).
8. D. M. Mayes, J. J. Kelly and J. B. Callis, in *Near Infra-red Spectroscopy: Bridging the Gap between Data Analysis and NIR Applications*, ed. by K. I. Hildrum, T. Isaksson, T. Naes and A. Tandberg, pp. 377–387, Ellis Horwood, Chichester (1992).
9. S. Bijlsma, D. J. Louwerse (Ad) and A. K. Smilde, *AIChE J.* **44**, 2713 (1998).
10. M. Maeder and A. D. Zuberbühler, *Anal. Chem.* **62**, 2220 (1990).

11. P. Bugnon, J. -C. Chottard, J. -L. Jestin, B. Jung, G. Laurenczy, M. Maeder, A. E. Merbach and A. D. Zuberbühler, *Anal. Chim. Acta*, **298**, 193 (1994).
12. R. M. Dyson, S. Kaderli, G. A. Lawrance, M. Maeder and A. D. Zuberbühler, *Anal. Chim. Acta*, **353**, 381 (1997).
13. S. Bijlsma, D. J. Louwerse (Ad), W. Windig and A. K. Smilde, *Anal. Chim. Acta*, **376**, 339 (1998).
14. B. Antalek and W. Windig, *J. Am. Chem. Soc.* **118**, 10 331 (1996).
15. W. Windig and B. Antalek, *Chemometrics Intell. Lab. Syst.* **37**, 241 (1997).
16. D. A. Burns and E. W. Ciurczak, *Handbook of Near-infrared Analysis*, Dekker, New York (1992).
17. J. J. Workman Jr, *Appl. Spectrosc. Rev.* **31**, 251 (1996).
18. E. Sanchez and B. R. Kowalski, *Anal. Chem.* **58**, 496 (1986).
19. G. A. F. Seber and C. J. Wild, *Nonlinear Regression*, Wiley, New York (1989).
20. R. A. Harshman and M. E. Lundy, *Comput. Statist. Data Anal.* **18**, 39 (1994).
21. A. K. Smilde, *Chemometrics Intell. Lab. Syst.* **15**, 143 (1992).
22. E. M. Hairfield, E. W. Moomaw, R. A. Tamburri and R. A. Vigil, *J. Chem. Educ.* **62**, 175 (1985).
23. J. Shao and D. Tu, *The Jackknife and Bootstrap*, Springer, New York (1995).
24. F. T. Chau and K. W. Mok, *Comput. Chem.* **16**, 239 (1992).
25. W. Windig, J. P. Hornak and B. Antalek, *J. Magn. Reson.* **132**, 298 (1998).
26. B. Antalek, J. P. Hornak and W. Windig, *J. Magn. Reson.* **132**, 307 (1998).
27. J. B. Kruskal, in *Multiway Data Analysis*, ed. by R. Coppi and S. Bolasco, pp. 7–18, Elsevier, Amsterdam (1989).
28. J. B. Kruskal, R. A. Harshman and M. E. Lundy, in *Multiway Data Analysis*, ed. by R. Coppi and S. Bolasco, pp. 115–122, Elsevier, Amsterdam (1989).
29. R. Bro and S. de Jong, *J. Chemometrics*, **11**, 393 (1997).
30. A. K. Smilde, R. Tauler, J. M. Henshaw, L. W. Burgess and B. R. Kowalski, *Anal. Chem.* **66**, 3345 (1994).

